Some approximate microfield distributions for multiply ionized plasmas: A critique

C. A. Iglesias* and C. F. Hooper, Jr.
University of Florida, Gainesville, Florida 32611

H. E. DeWitt
Lawrence Livermore National Laboratory, Livermore, California 94550
(Received 26 October 1982)

This paper provides a critical comparison of several approximate microfield distributions. Included are versions of the nearest-neighbor and next-nearest-neighbor approximations together with two approximations based on independent-perturber models. Where appropriate, results from a more complete theory will be used as reference. Monte Carlo results will be used in circumstances where the validity of the reference results are uncertain.

I. INTRODUCTION

The problem of calculating photoemission or photoabsorption by hot matter in regions where spectral lines play a significant role has long been of interest in astrophysics. Further interest has been generated in the subject by the development of high-powered lasers able to produce high-density plasmas in the laboratory. In order to provide reliable calculations a detailed knowledge of spectral line profiles is required. Since the computation of accurate line shapes is a major task, it is necessary to develop simple approximations suitable for large-scale numerical computations of opacities.

In relation to the line-shape problem several theories of electric microfield distributions have been proposed.[1-9] In the present paper we investigate some simple approximations to the microfield distributions. We present numerical calculations and compare them with more accurate theories and with each other. An analysis of these simple theories as applied to a range of plasma densities and temperatures, and to a variety of constituent compositions, is included.

Section II provides a general discussion of electric microfield distributions. Sections III–V deal with simple approximations to the microfield distribution. These are followed by a battery of numerical results presented in graphical form which are accompanied by appropriate observations and comments. A summary of results is provided.

II. GENERAL FORMALISM

We are interested in the electric microfield distribution function $Q(\vec{\epsilon})$ which is defined as the probability of finding an electric field $\vec{\epsilon}$, at a charged point located at $\vec{r}_0$, due to N particles contained in a volume Ω. The charge located at $\vec{r}_0$ is χe and each of the N particles carries a charge Ze; here e is the magnitude of the electron charge and χ and Z are positive integers. As a matter of convenience we will refer to the charged point at $\vec{r}_0$ as the zeroth particle. Then, if Z_{N+1} represents the configurational partition function for the N-particle system, we may write

$$Q(\vec{\epsilon})=\int\cdots\int d\vec{r}_0 d\vec{r}_1\cdots d\vec{r}_N e^{-\beta V}\delta(\vec{\epsilon}-\vec{E})/Z_{N+1}\ , \tag{2.1}$$

where $\vec{r}_j$ represents the coordinate of the jth particle, $\beta=(kT)^{-1}$, V represents the potential energy of the system, and $\vec{E}$ represents the electric field at $\vec{r}_0$ due to the N particles in a given coordinate configuration.

If we follow the usual practice of introducing an integral expression for $\delta(\vec{\epsilon}-\vec{E})$ we can rewrite Eq. (2.1) in the form

$$Q(\vec{\epsilon})=\frac{1}{2\pi^2\epsilon}\int_0^\infty dl\, lT(l)\sin(\epsilon l)\ , \tag{2.2}$$

where

$$T(l)=\frac{1}{Z_{N+1}}\int\cdots\int d\vec{r}_0 d\vec{r}_1\cdots d\vec{r}_N e^{-\beta V}e^{i\vec{l}\cdot\vec{E}}\ . \tag{2.3}$$

Further, if we specify that the system is isotropic, we can write

$$P(\epsilon)=\frac{2\epsilon}{\pi}\int_0^\infty dl\, lT(l)\sin(\epsilon l)\ , \tag{2.4}$$

where $P(\epsilon)$ and $Q(\vec{\epsilon})$ are related through the relation

$$4\pi Q(\vec{\epsilon})\epsilon^2 d\epsilon=P(\epsilon)d\epsilon\ . \tag{2.5}$$

We see then that the calculation of $P(\epsilon)$ involves the ensemble average of $\exp(i\vec{l}\cdot\vec{E})$ followed by the sine transform indicated in Eq. (2.4). To our knowledge the only reliable method to determine $P(\epsilon)$ for all plasma densities and temperatures is through the use of "computer experiments." However, such methods are expensive since they require large-scale numerical computations. In this paper the "accurate" theory mentioned in the Introduction refers to that of Hooper *et al.*[6,7] which has been shown to agree[8] well with Monte Carlo results for weakly and intermediately coupled plasmas.

Proceeding, we follow Mozer and Baranger[5] (MB) and distinguish two types of electric fields, a high-frequency and a low-frequency component. The distribution of the high-frequency component is calculated by considering a gas of ions interacting through a Coulomb potential and immersed in a uniform neutralizing background. The distribution of the low-frequency component is determined by considering a gas of ions interacting through an effective screened potential. The shielding of the ions in the latter case is a way to account for electron-screening ef-

 ©1983 The American Physical Society

fects since the electric fields due to ions vary slowly over times on the order of electron relaxation times. The effective potential is usually taken to be the Debye-Hückel[10] result, which applies to classical weakly coupled systems and long times. The present paper emphasizes the low-frequency distribution since it is this component of the electric microfield which is necessary as input in line-shape calculations.[11] In the formal development, however, there is little difference between the two components.

The potential energy and field appearing in Eq. (2.1) will differ for each distribution, although in both cases the potential energy is assumed to be given by the sum of pairwise interactions

$$V=\sum_{\substack{j=1\\ j>i}}^{N}\sum_{i=0}^{N} v(i,j)\ , \tag{2.6}$$

and the electric field by

$$\begin{aligned}&\vec{\mathrm{E}}=-(\chi e)^{-1}\vec{\nabla}_0 V=\sum_{j=1}^{N}\vec{\epsilon}(\vec{\mathrm{r}}_{10})\ ,\\ &\vec{\epsilon}(\vec{\mathrm{r}}_{10})=-(\chi e)^{-1}\vec{\nabla}_0 v(r_{10})\ ,\end{aligned} \tag{2.7}$$

where $\vec{\nabla}_0$ is the gradient with respect to $\vec{\mathrm{r}}_0$.

For the low-frequency case, the interaction potentials are given by

$$v(r_{ij})=\frac{Z^2e^2}{r_{ij}}e^{-r_{ij}/\lambda_D},\quad 0\neq i,j,\quad i<j \tag{2.8a}$$

$$v(r_{i0})=\frac{Z\chi e^2}{r_{i0}}e^{-r_{i0}/\lambda_D}\ , \tag{2.8b}$$

where the Debye length is $\lambda_D=(4\pi e^2 n_e\beta)^{1/2}$, the ion number density is $n=N/\Omega$, the electron number density is $n_e=N_e/\Omega$, and $\vec{\mathrm{r}}_{ij}=\vec{\mathrm{r}}_i-\vec{\mathrm{r}}_j$, $r_{ij}=|\vec{\mathrm{r}}_{ij}|$. Finally, since the dimensionless combination $\beta v(r_{ij})$ appears frequently, it is convenient to write Eq. (2.8) in revised form

$$\begin{aligned}\beta v(r_{ij})&=\frac{\beta Z^2e^2/R_0}{r_{ij}/R_0}\exp\left[-\frac{r_{ij}}{R_0}\frac{R_0}{\lambda_D}\right],\quad 0\neq i,j,\quad i<j\\ &=\frac{Z^2\Gamma_{0e}}{r_{ij}/R_0}\exp\left[-\sqrt{3\Gamma_{0e}}\left[\frac{r_{ij}}{R_0}\right]\right],\quad 0\neq i,j,\quad i<j\\ \beta v(r_{i0})&=\frac{Z\chi\Gamma_{0e}}{r_{ij}/R_0}\exp\left[-\sqrt{3\Gamma_{0e}}\left[\frac{r_{ij}}{R_0}\right]\right].\end{aligned} \tag{2.9}$$

Here, R_0 is the electron-sphere radius defined by

$$\tfrac{4}{3}\pi R_0^3 N_e=\Omega\ ,$$

and the plasma parameter Γ is given by

$$\Gamma=Z\chi\Gamma_{0e}=\frac{Z\chi\beta e^2}{R_0}\ .$$

Defining a new variable $x_{ij}=r_{ij}/R_0$, Eq. (2.9) can be written as

$$\begin{aligned}\beta v(x_{ij})&=\frac{Z^2\Gamma_{0e}}{x_{ij}}\exp(-\sqrt{3\Gamma_{0e}}x_{ij}),\quad 0\neq i,j,\quad i<j\\ \beta v(x_{i0})&=\frac{Z\chi\Gamma_{0e}}{x_{i0}}\exp(-\sqrt{3\Gamma_{0e}}x_{i0})\ .\end{aligned} \tag{2.10}$$

III. INDEPENDENT-PERTURBER MODEL

The independent-perturber-interaction model (IP model) for calculating microfield distributions neglects all interactions except those involving the zeroth particle. Lewis and Margenau[4] have used this model to calculate the high-frequency component distribution. Here, we extend the calculations to the low-frequency distribution.

In order to investigate the IP model we use the fact that the Fourier transform of the microfield distribution may be expressed as a quotient of two generalized configurational partition functions[8]

$$T(l)=Z_{N+1}(l)/Z_{N+1}(l=0)\ , \tag{3.1}$$

$$Z_{N+1}(l)=\int\cdots\int d\vec{\mathrm{r}}_0 d\vec{\mathrm{r}}_1\cdots d\vec{\mathrm{r}}_N e^{-\beta V(l)}\ , \tag{3.2}$$

and

$$V(l)=V-\beta^{-1}l\,\vec{\mathrm{l}}\cdot\vec{\mathrm{E}}\ . \tag{3.3}$$

Because $Z_{N+1}(l)$ may be interpreted as a configurational partition function for a system with potential energy $V(l)$, we are able to take advantage of the previous theories developed on this subject. In particular, we make use of the thermodynamic perturbation theory proposed by Zwanzig.[12] In what follows we concentrate on $Z_{N+1}(l)$ since Z_{N+1} is determined by setting $l=0$ in the expression for $Z_{N+1}(l)$.

The perturbation theory involves separating the potential energy into two parts

$$V(l)=V_0(l)+V_1(l)\ , \tag{3.4}$$

where $V_0(l)$ is the potential energy of an unperturbed (reference) system and $V_1(l)$ is the perturbation. With Eq. (3.4) we may write

$$Z_{N+1}(l)=Z^0_{N+1}(l)\langle e^{-\beta V_1(l)}\rangle_{0,l}\ , \tag{3.5}$$

where

$$\begin{aligned}Z^0_{N+1}(l)&=\int\cdots\int d\vec{\mathrm{r}}_0 d\vec{\mathrm{r}}_1\cdots d\vec{\mathrm{r}}_N e^{-\beta V_0(l)}\ ,\\ \langle f\rangle_{0,1}&=\int\cdots\int d\vec{\mathrm{r}}_0 d\vec{\mathrm{r}}_1\cdots d\vec{\mathrm{r}}_N e^{-\beta V_0(l)}\\ &\quad\times f/Z^0_{N+1}\ .\end{aligned} \tag{3.6}$$

Equations (3.4)–(3.6) provide us with some basic results concerning microfield distributions. In order to apply them, we must choose a reference system, and hence, specify $V_0(l)$ and $V_1(l)$. We note that although the separation of $V(l)$ in Eq. (3.4) is arbitrary, we require knowledge of the properties of the reference system if the method is to be useful; for example, the free energy and radial distribution function.

In the hope of gaining some insight into the problem of choosing a reference system we digress somewhat and consider a conjecture proposed by one of us (C.F.H).[6] We speculate that, in the calculation of microfield distributions, terms involving interactions between the zeroth particle and individual perturbers are more important than those terms where the interactions are between the N perturbers only. The former are referred to as central terms and the latter are the noncentral terms. The actual discrimination between central and noncentral terms is accomplished by separating the central ones into short- and

long-range parts. Each of these central parts is in turn treated by different expansion schemes. It can be shown by straightforward manipulation that the formalisms developed by Hooper *et al.*[6–8] are equivalent to the following: Let the reference system in Eq. (3.4) consist of all noncentral plus all long-range central terms and the perturbation of all the short-range central terms. Proceed by treating the reference system in a Debye-chain expansion[13] followed by a rapidly convergent virial expansion of the perturbation.[6–8]

Suppose we carry the above conjecture to an extreme. We assume that the central terms contain most of the relevant information, while the noncentral terms are weak and almost unimportant. Here, weak is to be interpreted not in the usual sense, as described by a small plasma parameter for example, but instead as having a very small effect on the final result. If this point of view is correct, then we are justified in formulating an alternative reference system that consists of all of the central contributions; that is, the reference system is given by the IP model. The validity of our assumption, and consequently of our choice for $V_0(l)$, may be ascertained from Figs. 5–8, where it is shown that the IP model is in reasonable agreement with the results of Hooper *et al.*,[6,7] especially in cases where $\chi > Z$.

Now let us examine the implications of the preceding discussion. First, the separation of $V(l)$ is given by

$$V_0(l)=\sum_{j=1}^{N} v(0,j)-\frac{i\vec{l}}{\beta}\cdot\vec{\mathrm{E}} \quad \text{(which equals all central terms)}, \tag{3.7}$$

$$V_1(l)=V_1=\sum_{\substack{j=2\\ j>1}}^{N}\sum_{i=1}^{N} v(i,j) \quad \text{(which equals all noncentral terms)}.$$

Substitution of Eq. (3.7) into Eqs. (3.1)–(3.6) yields

$$T(l)=T_{\mathrm{IP}}(l)(\langle e^{-\beta V_1}\rangle_{0,l}/\langle e^{-\beta V_1}\rangle_{0,0}) , \tag{3.8}$$

where

$$T_{\mathrm{IP}}(l)=\exp\left[4\pi n\int_0^\infty dr_{10}r_{10}^2 e^{-\beta v(r_{10})}\times\left[\frac{\sin[l\epsilon(r_{10})]}{l\epsilon(r_{10})}-1\right]\right] , \tag{3.9}$$

$$\epsilon(r_{j0})=|\vec{\epsilon}(\vec{r}_{j0})| . \tag{3.10}$$

By means of our conjecture, we assume V_1 to be weak and expand Eq. (3.8) in terms of the Thiele's semi-invariants or cumulants,

$$\frac{\langle e^{-\beta V_1}\rangle_{0,l}}{\langle e^{-\beta V_1}\rangle_{0,0}}=\exp[-\beta(\langle V_1\rangle_{0,l}-\langle V_1\rangle_{0,0})+\cdots] , \tag{3.11}$$

where the ellipsis represents the higher-order cumulants. We shall restrict the rest of the analysis to the first-order cumulants.

At this point we differentiate between high- and low-frequency microfields, and concentrate on the latter. Now, the pairwise-additive form of V_1 for the low-frequency component allows us to write

$$\langle V_1\rangle_{0,l}-\langle V_1\rangle_{0,0}=\frac{n^2}{2}\int d\vec{r}_1 d\vec{r}_2 v(r_{12})\times[g_0(\vec{r}_1,\vec{r}_2;l)-g_0(\vec{r}_1,\vec{r}_2;0)] . \tag{3.12}$$

In Eq. (3.12), $g_0(\vec{r}_1,\vec{r}_2;l)$ is the radial distribution function in the reference system

$$g_0(\vec{r}_1,\vec{r}_2;l)=\frac{\Omega^2}{Z^0_{N+1}(l)}\int\cdots\int d\vec{r}_0 d\vec{r}_3\cdots d\vec{r}_N e^{-\beta V_0(l)} \tag{3.13}$$

$$=1+\frac{1}{\Omega}\int d\vec{r}_0 f(\vec{r}_{10};l)f(\vec{r}_{20};l) , \tag{3.14}$$

where

$$f(\vec{r}_{j0};l)=\exp[-\beta v(r_{j0})+i\vec{l}\cdot\vec{\epsilon}(\vec{r}_{j0})]-1 . \tag{3.15}$$

The simple result in Eq. (3.14) is a direct consequence of choosing the IP model as the reference system. Observe that the potentials appearing in Eqs. (3.12)–(3.15) are shielded Coulomb interactions, given by Eq. (2.8). Substitution of Eq. (3.14) into (3.12) yields

$$\langle V_1\rangle_{0,l}-\langle V_1\rangle_{0,0}=16\pi^2 n^2\sum_{k=0}^{\infty}(-1)^k(2k+1)\int_0^\infty dr_{10}r_{10}^{3/2}K_{k+1/2}(r_{10}/\lambda_D)\times\int_0^{r_{10}} dr_{20}r_{20}^{3/2}I_{k+1/2}(r_{20}/\lambda_D)\times\{[e^{-\beta v(r_{10})}j_k(l\epsilon(r_{10}))-\delta_{k,0}][e^{-\beta v(r_{20})}j_k(l\epsilon(r_{20}))-\delta_{k,0}] -\delta_{k,0}(e^{-\beta v(r_{10})}-1)(e^{-\beta v(r_{20})}-1)\} . \tag{3.16}$$

The functions I and K refer to modified Bessel functions of the first and third kind, respectively, while j_k specifies a spherical Bessel function of order k.[14] In obtaining Eq. (3.16) we expanded $v(r_{12})$ in terms of Legendre polynomials P_k

$$v(r_{12})=\sum_{k=0}^{\infty}(2k+1)v_k(r_{10},r_{20})P_k(\mu) ,$$

$$v_k(r_{10},r_{20})=\tfrac{1}{2}\int_{-1}^{1} d\mu\, v(r_{12})P_k(\mu) ,$$

and

$$\mu=\frac{\vec{r}_{10}\cdot\vec{r}_{20}}{r_{10}r_{20}} . \tag{3.17}$$

The coefficients $v_k(r_{10},r_{20})$, which can be evaluated explicitly, have the form[15]

$$v_k(r_{10},r_{20})=\frac{Z^2e^2}{kT}K_{k+1/2}(r_{10}/\lambda_D)I_{k+1/2} \times(r_{20}/\lambda_D)/(r_{10},r_{20})^{1/2} , \quad r_{10}>r_{20} \tag{3.18}$$

where λ_D in Eq. (3.18) refers to electron screening.

The double integral in Eq. (3.16) is of a particularly tractable form. In fact, it is formally similar to the second term in the Mozer and Baranger[5] scheme except that in Ref. 5 all interactions are screened by ions and electrons while here they are screened by electrons only. The same difference exists between Eq. (3.9) and the first term in the Mozer and Baranger[5] expansion.

IV. NEAREST-NEIGHBOR APPROXIMATION

The nearest-neighbor (NN) approximation to the microfield distribution assumes that the electron field at $\vec{r}_0$ is dominated by that of the nearest neighbor. The usual derivation, based solely on heuristic arguments, is given in many places; see, for example, Lewis and Margenau.[4] Here we choose another approach which we believe provides additional insight. With the NN assumption the expression for $P(\epsilon)$ can be written as

$$P(\epsilon)=4\pi\epsilon^2 n\int d\vec{r}_1 P(r_{10})\delta(\vec{\epsilon}-\vec{\epsilon}(\vec{r}_{10})) , \tag{4.1}$$

where $nP(r_{10})d\vec{r}_{10}$ is the probability that the NN (the particle closest to $\vec{r}_0$) is in $d\vec{r}_{10}$ at $\vec{r}_{10}$. $P(r_{10})$ may be expressed in terms of an ensemble average

$$P(r_{10})=\frac{\Omega^2}{Z_{N+1}}\int\cdots\int d\vec{r}_2\cdots d\vec{r}_N e^{-\beta V}\times\prod_{j=2}^{N}\Theta(r_{j0}-r_{10}) , \tag{4.2}$$

$$\Theta(y)=\begin{cases}1, & y\geq 0\\ 0, & y<0 .\end{cases}$$

The Θ functions appearing in Eq. (4.2) guarantee that the particle at $\vec{r}_1$ is indeed the NN of the zeroth particle.

The evaluation of Eq. (4.2) is difficult except within the framework of some approximation. For example, in the IP model $P(r_{10})$ simplifies considerably to

$$P(r_{10})\underset{\text{IP}}{\rightarrow}e^{-\beta v(r_{10})}\times\exp\left[-4\pi n\int_0^{r_{10}}dr_{20}r_{20}^2e^{-\beta v(r_{20})}\right] \tag{4.3}$$

a result previously obtained by Lewis and Margenau.[4] In an effort to take into account the effects of the interactions between the N particles, it has been common practice[16] to replace the factors $\exp(-\beta v)$ in Eq. (4.3) by the exact radial distribution functions

$$P(r_{10})\simeq P_0(r_{10})\equiv g(r_{10})e^{-N(r_{10})} , \tag{4.4}$$

$$N(r_{10})=4\pi n\int_0^{r_{10}}dr_{20}r_{20}^2g(r_{20}) , \tag{4.5}$$

with $g(r_{j0})$ the radial distribution function defined by Eq. (4.11). The simple result in Eq. (4.3) may be interpreted as follows: $P(r_{10})\,|_{\text{IP}}$ is asymptotically the product of the probability of finding a particle at $\vec{r}_1$ given that the zeroth particle is at $\vec{r}_0$ and the probability that there are no particles within a sphere of radius r_{10} centered at $\vec{r}_0$. This interpretation is possible since the two probabilities are independent in the IP model. However, if the interactions between the N particles are not neglected, then the product of these probabilities are no longer independent. Therefore, in the remainder of this section we will examine the validity of Eq. (4.4).

We return to the previous given definition of $P(r_{10})$ and observe that the effect of the Θ functions may be simulated by placing a hard core of radius r_{10} centered about the zeroth particle. That is,

$$P(r_{10})=\Omega^2\int\cdots\int d\vec{r}_2\cdots d\vec{r}_N e^{-\beta V^*}/Z_{N+1} \tag{4.6}$$

or,

$$nP(\vec{r}_{10})=N\int\cdots\int d\vec{r}_2\cdots d\vec{r}_N e^{-\beta V^*}/Z_N , \tag{4.7}$$

where we have introduced the potential V^* defined by

$$V^*\equiv V+\Phi ,$$

$$\Phi=\sum_{j=2}^{N}\phi(r_{j0}) ,$$

and

$$\phi(r_{j0})=\begin{cases}\infty, & r_{j0}\leq r_{10}\\ 0, & r_{j0}>r_{10} .\end{cases} \tag{4.8}$$

A cluster expansion for Eq. (4.7) may be accomplished by introducing the Mayer functions

$$\chi(r)=(e^{-\beta\phi(r)}-1) . \tag{4.9}$$

Then, with the help of Eq. (4.9) we can write Eq. (4.7) in the form

$$nP(\vec{r}_{10})=ng(\vec{r}_{10})+n^2\int d\vec{r}_2 g(\vec{r}_{10},\vec{r}_{20})\chi(\vec{r}_{20}) +\frac{n^3}{2}\int d\vec{r}_2 d\vec{r}_3 g(\vec{r}_{10},\vec{r}_{20},\vec{r}_{30})\chi(\vec{r}_{20})\chi(\vec{r}_{30})+\cdots =ng(\vec{r}_{10})\exp\left[\sum_{j=1}^{N-1}\frac{n^j}{j!}\beta_j(\vec{r}_{10})\right] . \tag{4.10}$$

In Eq. (4.10) the g's are the reduced distribution functions

$$n^s g(\vec{r}_{10},\ldots,\vec{r}_{30}) =\frac{N!}{(N-s)!}\int d\vec{r}_{s+1}\cdots d\vec{r}_N e^{-\beta V}/Z_{N+1} ; \tag{4.11}$$

the β_j's are cluster integrals defined as

$$\beta_j(\vec{r}_{10})=\int d\vec{r}_2\cdots d\vec{r}_{j+1}U_j(\vec{r}_{20},\ldots,\vec{r}_{j+1,0}) \times\chi(\vec{r}_{20})\cdots\chi(\vec{r}_{j+1,0}) , \tag{4.12}$$

where the functions U_j are obtained by inverting the following Ursell expansion[17]:

$$g(\vec{r}_{10},\vec{r}_{20})g^{-1}(\vec{r}_{10})=U_1(\vec{r}_{20}) ,$$
$$g(\vec{r}_{10},\vec{r}_{20},\vec{r}_{30})g^{-1}(r_{10})=U_1(\vec{r}_{20})U_1(\vec{r}_{30}) + U_2(\vec{r}_{20},\vec{r}_{30}) , \quad (4.13)$$

and so on.

Equation (4.10) gives an expression for $P(\vec{r}_{10})$ in terms of the radial distribution function plus corrections. The corrections are due to the exlcuded volume effects of the Θ functions.

The virial expansion in Eq. (4.10) is valid for systems whose pair interactions are short ranged, such as a shielded Coulomb potential. For Coulomb systems, with their long-range interactions, the virial expansions diverge term by term and a "renormalization" procedure is necessary. Such a procedure has been described in detail by Salpeter[13] who proposed an expansion in the plasma parameter instead of the density. In addition to the plasma parameter the evaluation of Eq. (4.10) involves the length parameter r_{10} which may be interpreted as an effective hard-sphere radius of the zeroth particle. Consequently, we introduce an effective packing fraction η

$$\eta=\tfrac{4}{3}\pi r_{10}^3 n . \quad (4.14)$$

An expansion in terms of η is now possible, provided that η is sufficiently small. However, the parameter η is not necessarily small since it clearly depends on r_{10} which can vary from zero to infinity. Therefore, the value of such an expansion is limited: limited to situations where η is small. But it is this very limitation which is necessary to assure the validity of the approximation in Eq. (4.5).

Proceed by noting that the $\chi(\vec{r}_{j0})$ occurring in the cluster integrals $\beta_j(\vec{r}_{10})$ restrict the range over $\vec{r}_j$ to a sphere of radius r_{10} centered at $\vec{r}_j$. Thus, make the transformation to the dimensionless variable

$$\vec{u}=\vec{r}/r_{10} \quad (4.15)$$

and consequently obtain,

$$\beta_j(\vec{r}_{10})=\left[\frac{3\eta}{4\pi}\right]^j \int d\vec{u}_2\cdots d\vec{u}_{j+1} \times U_j(r_{10}\vec{u}_{20},\ldots,r_{10}\vec{u}_{j+1,0}) \times\chi(\vec{u}_{20})\cdots\chi(\vec{u}_{j+1}) . \quad (4.16)$$

For small enough r_{10}, such that $\eta\ll 1$, we can write

$$P(\vec{r}_{10})=g(\vec{r}_{10})\exp\left[\frac{3\eta}{4\pi}\int d\vec{u}\, U_1(r_{10}\vec{u})\chi(\vec{u}) + O(\eta^2)\right] , \quad (4.17)$$

which reduces to $P_0(\vec{r}_{10})$ to first order in η only after some additional approximations, e.g., if

$$g(\vec{r}_{10},\vec{r}_{20})\cong g(\vec{r}_{10})g(\vec{r}_{20})g(\vec{r}_{12}) \quad (4.18)$$

and

$$g(\vec{r}_{12})\cong 1 . \quad (4.19)$$

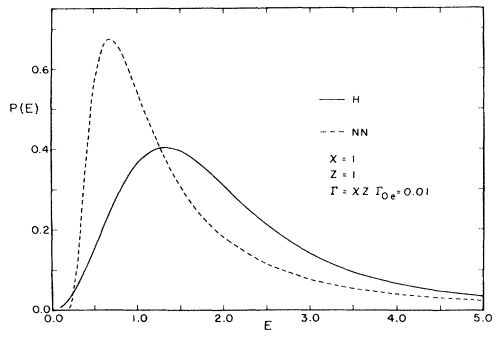

FIG. 1. NN microfield distribution function $P(E)$ is compared with the results of a more complete calculation labeled H (Hooper). All ionic constituents are singly charged. Field variable is dimensionless; $E=\epsilon/\epsilon_0$, where ϵ_0 is the normal field strength e/R_0^2. R_0 is the "ion-sphere radius" for electrons (hereafter referred to as the electron-sphere radius), not ions.

This development explicitly serves to demonstrate how restrictive the approximation appearing in Eq. (4.5) really is.

V. NEXT-NEAREST NEIGHBOR

The next-nearest-neighbor (NNN) approximation tries to improve on the results of the previous section by including the electric field due to the second-nearest neighbors, as well. Hence,

$$P(\epsilon)=2\pi\epsilon^2 n^2\int d\vec{r}_1 d\vec{r}_2\,\delta(\vec{\epsilon}-\vec{\epsilon}(\vec{r}_{10})-\vec{\epsilon}(\vec{r}_{20})) \times H(\vec{r}_{10},\vec{r}_{20}) \quad (5.1)$$

with $n^2H(\vec{r}_{10},\vec{r}_{20})d\vec{r}_1 d\vec{r}_2$ representing the probability that the two NN are in $d\vec{r}_1$ at $\vec{r}_1$ and $d\vec{r}_2$ at $\vec{r}_2$. In terms of an ensemble average we have

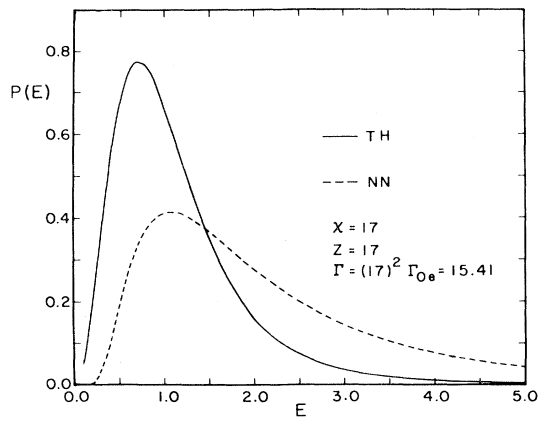

FIG. 2. NN microfield distribution function $P(E)$ is compared with the results of a more complete calculation labeled TH (Tighe and Hooper). All ionic constituents are 17 times charged. Field variable E is dimensionless; $E=\epsilon/\epsilon_0$, where $\epsilon_0=e/R_0^2$ and R_0 in the electron-sphere radius.

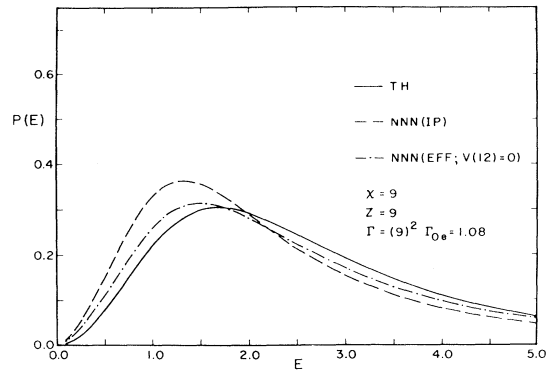

FIG. 3. A comparison of microfield distribution calculated with two versions of the NNN approximation, with the result of a more complete TH calculation. All ionic constituents are 9 times ionized. Field variable E is dimensionless, scaled in terms of the electron-sphere radius.

$$H(\vec{r}_{10},\vec{r}_{20})=\frac{\Omega^3}{Z_{N+1}}\int\cdots\int d\vec{r}_3\cdots d\vec{r}_N e^{-\beta V}\times\prod_{j=3}^{N}\Theta(r_{j0}-R)\,, \tag{5.2}$$

$$R=\max\{r_{10},r_{20}\}\,. \tag{5.3}$$

Without any approximation, we may rewrite Eq. (5.1) in the form

$$P(\epsilon)=\frac{2\epsilon}{\pi}\int_0^\infty dl\, l\sin(\epsilon l)T(l)\,, \tag{5.4}$$

where

$$T(l)=\frac{n^2}{2}\int d\vec{r}_1 d\vec{r}_2 H(\vec{r}_{10},\vec{r}_{20})\exp\{i\vec{l}\cdot[\vec{\epsilon}(\vec{r}_{10})+\vec{\epsilon}(\vec{r}_{20})]\}$$
$$=8\pi^2 n^2\int_0^\infty dr_{10}r_{10}^2\int_0^\infty dr_{20}r_{20}^2\sum_{k=0}^{\infty}(-1)^k(2k+1)j_k(l\epsilon(r_{10}))j_k(l\epsilon(r_{20}))H_k(r_{10},r_{20})\,, \tag{5.5}$$

and

$$H_k(r_{10},r_{20})=\tfrac{1}{2}\int_{-1}^{1}d\mu\, H(\vec{r}_{10},\vec{r}_{20})P_k(\mu)\,,$$
$$\mu=\frac{\vec{r}_{10}\cdot\vec{r}_{20}}{r_{10}r_{20}}\,. \tag{5.6}$$

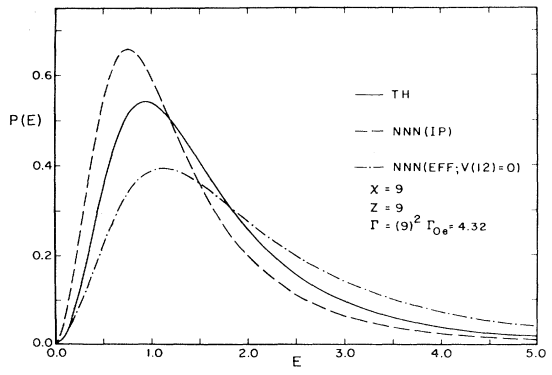

FIG. 4. A comparison of microfield distribution calculated with two versions of the NNN approximation, with the result of a more complete TH calculation. All ionic constituents are 9 times ionized. Field variable E is dimensionless, scaled in terms of the electron-sphere radius.

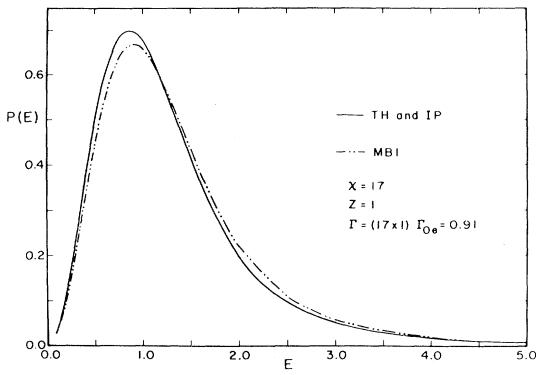

FIG. 5. A comparison of microfield distributions calculated with two many-body approximations IP and MB 1, with results from a more complete many-body theory TH. IP results include only electron screening of the ion whereas MB 1 includes some ion as well as electron screening. There is an ion at the origin with a 17 + charge, but the perturbers are singly charged. Field variable is in dimensionless units scaled in terms of the normal electron field at the origin.

The evaluation of Eq. (5.5) requires knowledge of $H(\vec{r}_{10},\vec{r}_{20})$, which in general, is difficult to evaluate. In the IP approximation $H(\vec{r}_{10},\vec{r}_{20})$ is given by

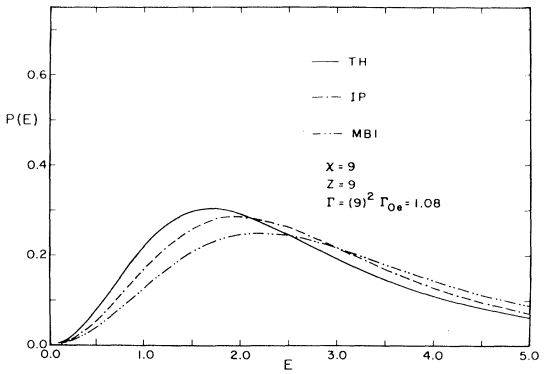

FIG. 6. A comparison of microfield distributions calculated with two many-body approximations IP and MB 1, with results from a more complete theory TH. IP results include only electron screening of the ion whereas MB 1 includes some ion as well as electron screening. All ionic species have a charge of 9 + . Field variable is in dimensionless units in terms of the electron-sphere radius.

$$H(\vec{r}_{10},\vec{r}_{20}) \underset{\text{IP}}{\rightarrow} \exp\{-\beta[v(r_{10})+v(r_{20})]\} \times \exp\left[-4\pi n \int_0^R dr_{30} r_{30}^2 e^{-\beta v(r_{30})}\right] \quad (5.7)$$

and, as in Sec. IV, the effects of the interactions between the N particles may be approximated in an *ad hoc* fashion by

$$H(\vec{r}_{10},\vec{r}_{20}) \simeq H_0(\vec{r}_{10},\vec{r}_{20}) = g_2(\vec{r}_{10},\vec{r}_{20}) e^{-N(R)} \quad (5.8)$$

with $g_2(\vec{r}_{10},\vec{r}_{20})$ the triplet correlation function defined by Eq. (4.11). The approximation in Eq. (5.8) suffers from the same difficulties as $P_0(r_{10})$ in Eq. (4.5); they both neglect the excluded volume effects of the Θ functions. The discussion concerning the validity of $H_0(\vec{r}_{10},\vec{r}_{20})$ follows along the same lines already presented for $P_0(r_{10})$.

In an effort to obtain simple expressions for $P(\epsilon)$ which are suitable for opacity computations, we assume Eq. (5.8) to be valid. But even with this approximation the calculation of Eqs. (5.4)—(5.6) is formidable. Furthermore, we require knowledge of the triplet correlation function $g_2(\vec{r}_{10},\vec{r}_{20})$. This last difficulty may be dealt with by introducing the Kirkwood superposition approximation[18]

$$g_2(\vec{r}_{10},\vec{r}_{20}) \simeq g(r_{10}) g(r_{20}) g(r_{12}) \, . \quad (5.9)$$

Weisheit and Pollock[16] have indicated that the superposition approximation may be adequate for evaluating microfield distributions. Hence, with approximations (5.8) and (5.9) we obtain for Eqs. (5.5) and (5.6),

$$T(l) \simeq 16\pi^2 n^2 \int_0^\infty dr_{10} r_{10}^2 g(r_{10}) e^{-N(r_{10})} \int_0^{r_{10}} dr_{20} r_{20}^2 g(r_{20}) \sum_{k=0}^{\infty} (-1)^k (2k+1) j_k(l\epsilon(r_{10})) j_k(l\epsilon(r_{20})) g^{(k)}(r_{10},r_{20}) \quad (5.10)$$

with

$$g^{(k)}(r_{10},r_{20}) = \tfrac{1}{2} \int_{-1}^{1} d\mu \, g(r_{12}) P_k(\mu) \, . \quad (5.11)$$

Equation (5.10) simplifies considerably if we neglect correlations between particles 1 and 2,

$$g(r_{12}) \simeq 1 \, , \quad (5.12)$$

and consequently,

$$g^{(k)}(r_{10},r_{20}) \simeq \begin{cases} 1, & k=0 \\ 0, & \text{otherwise} \, . \end{cases} \quad (5.13)$$

Although the quantitative effects of approximation (5.12) are not known, qualitatively it gives, on the average, too high a value for the electric field at $\vec{r}_0$ and consequently a $P(\epsilon)$ calculation which neglects correlations between the two NN is expected to peak at a value of ϵ that is too large. Substitution of Eq. (5.12) into (5.10) and subsequent substitution of Eq. (5.10) into Eq. (5.4) yields

$$P(\epsilon) \simeq 32\epsilon\pi^2 n^2 \int_0^\infty dr_{10} r_{10}^2 \frac{g(r_{10}) e^{-N(r_{10})}}{\epsilon(r_{10})} \int_0^{r_{10}} dr_{20} r_{20}^2 \frac{g(r_{20}) B(r_{10},r_{20})}{\epsilon(r_{20})} \, , \quad (5.14)$$

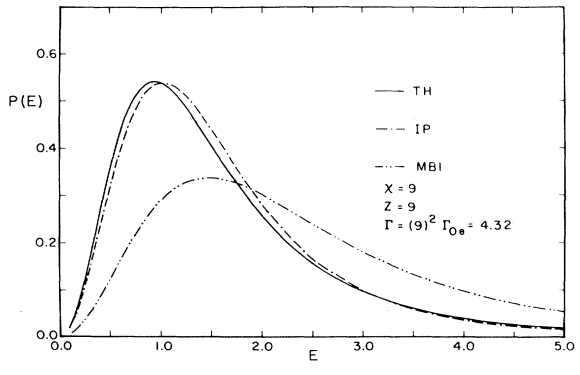

FIG. 7. A comparison of microfield distributions calculated with two many-body approximations IP and MB 1 with results from a more complete theory TH. IP results include only electron screening of the ions whereas the MB 1 includes some ion as well as electron screening. All ionic species have a charge of $9+$. Field variable is in dimensionless units in terms of the electron-sphere radius.

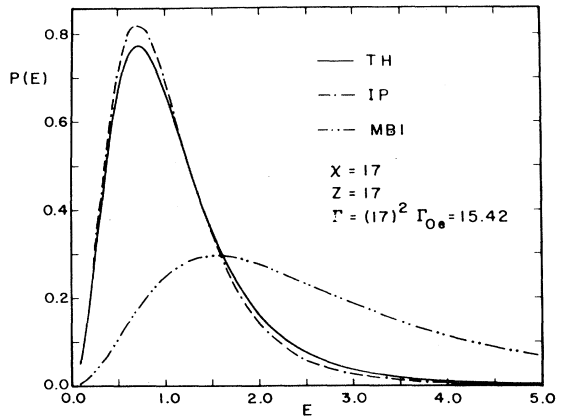

FIG. 8. A comparison of microfield distributions calculated with two many-body approximations IP and MB 1 with results from a more complete theory TH. IP results include only electron screening of the ions whereas the MB 1 includes some ion as well as electron screening. All ionic species have a charge of $17+$. Field variable is in dimensionless units in terms of the electron field at the origin.

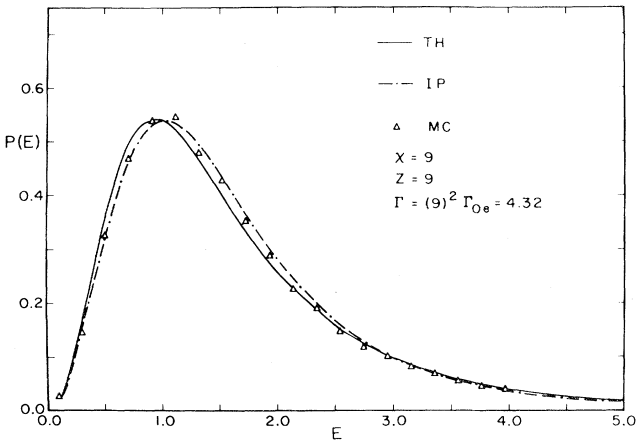

FIG. 9. A comparison of the microfield distributions calculated with IP and TH methods with MC results. All ionic constituents carry a charge of 9 + . Dimensionless field variable is scaled in terms of the electron-sphere radius.

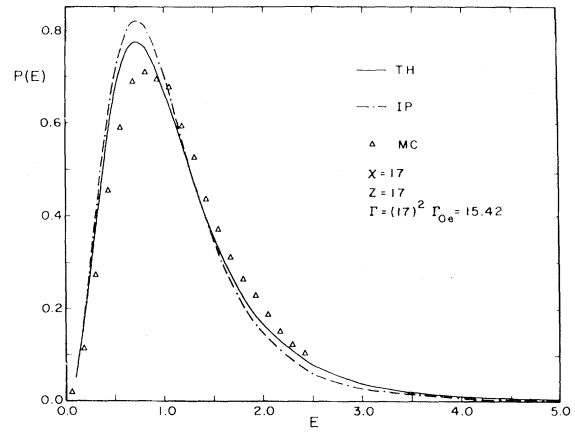

FIG. 10. A comparison of the microfield distributions calculated with IP and TH methods with MC results. All ionic constituents carry a charge of 17 + . Dimensionless field variable is scaled in terms of the electron-sphere radius.

where

$$B(r_{10},r_{20})=\begin{cases}0, & \epsilon<\epsilon(r_{20})-\epsilon(r_{10}) \text{ or } \epsilon>\epsilon(r_{20})+\epsilon(r_{10})\\ 1, & \epsilon=\epsilon(r_{20})-\epsilon(r_{10}) \text{ or } \epsilon=\epsilon(r_{20})+\epsilon(r_{10})\\ 2, & \epsilon(r_{20})-\epsilon(r_{10})<\epsilon<\epsilon(r_{20})+\epsilon(r_{10})\ .\end{cases} \tag{5.15}$$

The results in Eqs. (5.14) and (5.15) are of a particularly tractable form.

It is easily seen from Eq. (5.12) that applying the IP approximation to $H(\vec{r}_{10},\vec{r}_{20})$ is actually redundant. Therefore, substitution of Eq. (5.7) into Eq. (5.5) yields Eq. (5.14) except for all radial distribution functions in the Eq. (5.14) are replaced by the factors $\exp(-\beta v)$. Both results, Eq. (5.14) with appropriate $g(r)$ factors or with the exponential factors appropriate for the IP approximation, will be used later in Sec. VI to obtain numerical results.

VI. NUMERICAL RESULTS

In this section we compare ion microfield distributions generated using the various approximations introduced in the preceding sections with corresponding results produced with the aid of a more complete procedure. In addition, where available, comparisons are made with Monte Carlo (MC) results—computer simulations. Finally, we emphasize that a variety of plasma conditions and compositions are surveyed.

Before considering detailed analysis we want to describe a general feature that appears to be common to all the approximations considered. As the value of the plasma parameter is increased from small to larger values, the approximation curves "move through" the more complete result (and also through the MC results). Hence, the NN results for low values of Γ have a peak that is significantly higher than the correct result and shifted to smaller field values. However, as the value of Γ increases, the NN peak drops below that of the more exact results and the difference in the position of the peaks decreases. For the NNN results, the behavior is similar, the primary difference being a decreased rate at which the relative positions of the curves change with a corresponding increase in Γ. The IP model also shows a similar behavior, but the transition is from the opposite direction and at a still slower rate.

The version of the NN approximation that has been studied is the one commonly used, Eqs. (4.4) and (4.5): a radial distribution function is employed in its calculation in place of a Boltzmann factor. Because of its simplicity and the plausable nature of its heuristic derivation, this version of the NN approximation is widely used. One purpose of this paper is to point out and illustrate the deficiencies of this method; for example, it always yields an incorrect weak-coupling limit. The magnitude of this problem is indicated in Fig. 1. Furthermore, as shown in Fig. 2, it cannot be counted on to yield good strong-coupling results either. Of course, in an intermediate region, there may be fortuitous agreement.

Two versions of the NNN approximations are considered, both of which neglect correlations between the two neighbors. The difference between the two lies in the nature of the interactions between the zeroth particle and each perturber: one version uses interactions which include ion and electron screening while the other has only electron screening. As seen in Figs. 3 and 4, these versions can lead to considerably different results, although neither generates a useful approximation over the entire range of plasma parameters considered here. The weak- and strong-coupling results are again in error although the rate of change with plasma parameter is less than that encountered with the NN results. The inclusion of interneighbor correlations will not improve matters.

The last set of approximations considered also has two subcategories: the independent perturber model IP discussed in Sec. III, and the MB 1 model which uses only the first term of the Mozer-Baranger theory.[5] Although both of these models involve perturbers acting independently of one another, the IP model uses interactions screened by electrons only, whereas the MB 1 model employs interactions screened by electrons *and* ions. The

MB 1 model can be generated by replacing the Boltzmann factor appearing in Eq. (3.9) by a radial distribution function, the Debye-Hückel approximation, in which screening due to both electrons and ions is included. The resulting expression $T_{\mathrm{MB}1}(l)$ can be used to calculate $P(\epsilon)$ in the MB 1 approximation. As seen from Figs. 5—8 the IP model approximates the more complete calculation over a wide range of plasma conditions. Interestingly, the IP model is always superior to the MB 1 model. Also, it should be noted that the least accurate application of the IP model occurs when it is applied to intermediately coupled cases, e.g., Fig. 6.

Finally, we discuss Figs. 9 and 10 which compare MC results with IP and reference calculations. These cases correspond to very strongly coupled plasmas. Figure 9 corresponds to an effective plasma parameter Γ of ~ 4 and in Fig. 10, the value of $\Gamma \sim 15$. The agreement in Fig. 9 between all curves may well be acceptable for many purposes. In Fig. 10, the agreement has worsened, but is still surprisingly close when the perturbative nature of the analytic theory is considered.

VII. CONCLUSIONS

For the range of plasma parameters considered in this paper, it is clear that the IP model is markedly superior to either the NN or NNN models. Its weak-coupling behavior is excellent and it also provides accurate representations of many situations where the constituent ions are strongly coupled. Its worst results occur for intermediate values of the plasma parameter as seen in Fig. 6. However, even here the IP approximation may provide results that are sufficiently accurate for many purposes.

On the other hand, the NN approximation is seldom valid. Hence, its use may lead to conclusions that are not even qualitatively correct. In any event, considerable caution must be exercised in the use of this approximation. Finally, while the NNN approximation is found to have deficiencies similar to those encountered with the NN model, its region of validity is different and somewhat extended.

A final implication of the preceding comments is that any approximation to the microfield distribution function that is successful over a significant range of plasma parameters must be a many-body calculation as opposed to one based on a few-body treatment.

ACKNOWLEDGMENTS

This work was supported in part by contracts from the U.S. Department of Energy and the Lawrence Livermore National Laboratory. The work of H. E. DeWitt is also supported by the Office of Naval Research.

---

*Present address: Department of Mathematics, Rutgers University, New Brunswick, N.J. 08903.

[1]J. Holtsmark, Ann. Phys. (N.Y.) 58, 577 (1919).
[2]A. A. Broyles, Phys. Rev. 100, 1181 (1955).
[3]G. Ecker, Z. Phys. 148, 593 (1957).
[4]M. Lewis and H. Margenau, Phys. Rev. 109, 842 (1958); Rev. Mod. Phys. 31, 569 (1959).
[5]M. Baranger and B. Mozer, Phys. Rev. 115, 521 (1969); 118, 626 (1960).
[6]C. F. Hooper, Jr., Phys. Rev. 149, 77 (1966); 165, 215 (1968).
[7]R. J. Tighe and C. F. Hooper, Phys. Rev. A 15, 1773 (1977).
[8]C. A. Iglesias and C. F. Hooper, Phys. Rev. A 25, 1049 (1982).
[9]C. A. Iglesias, Phys. Rev. A 27, 2705 (1983).
[10]P. Debye and E. Hückel, Z. Phys. 24, 185 (1923).
[11]M. Baranger, Atomic and Molecular Processes, edited by D. R. Bates (Academic, New York, in press).
[12]R. W. Zwanzig, J. Chem. Phys. 22, 1420 (1954).
[13]E. E. Salpeter, Ann. Phys. (N.Y.) 5, 183 (1958).
[14]The Bateman Manuscript Project, *Higher Transcendental Functions,* edited by A. Erdéyi (California Institute of Technology, Pasadena, California, 1953), Vol. II.
[15]W. J. Swiatecki, Proc. R. Soc. London Ser. A 205, 238 (1951).
[16]For example, C. F. Hooper, Jr., Phys. Rev. 169, 193 (1968); J. C. Weisheit and E. L. Pollock, *Spectral Line Shapes,* edited by B. Wende (de Gruyter, Berlin, 1981).
[17]H. D. Ursell, Proc. Cambridge Philos. Soc. 23, 685 (1927).
[18]J. G. Kirkwood, J. Chem. Phys. 3, 300 (1935).